CROSS-CORRELATION LASER SCATTERING

Z. KAM
Polymer Department, Weizmann Institute of Science, Rehovot, Israel

R. RIGLER
Medical Biophysics, Karolinska Institute, Stockholm, Sweden

ABSTRACT Cross-correlation between two detectors was applied to analyze laser light-scattering fluctuations. Laser scattering from random concentration fluctuations is spatially coherent over small angular areas that are inversely proportional in size to the dimension of the scattering volume. By cross-correlating scattering intensity fluctuations in different angles, the correlation due to relaxation of concentration fluctuations is practically eliminated, and correlations reflecting changes in the scattering from the individual particles can be enhanced. Rotational diffusion of assymetric particles, conformational relaxation of random coils, and association-dissociation dynamics are determined here using the above approach.

I. INTRODUCTION

In the last decade quasi-elastic laser light scattering (QELS), or as it is sometimes called, dynamic light scattering, has added the time dimension to the classic probe of incoherent, total-intensity scattering of light. Intensive work has been devoted to the analysis of the dynamics of different processes that contribute to fluctuation in intensity of the scattered light (references 1–3 are books reviewing the field). Indeed, experiments established the effect of diffusion on broadening and of directed motion on the Doppler shift of the spectrum of light scattered from a wide range of particle sizes and shapes. Today, QELS is routinely used for accurate measurements of translational diffusion coefficients of macromolecules in solution, and for anemometric measurements of linear and turbulent flow.

On the other hand, after theoretical analysis, a substantial effort by several experimenters was devoted to extract additional contributions to the observed dynamic fluctuations of coherent scattering. Still, the separation of the different contributions to the observed QELS spectrum is far from being straightforward. For small molecules, the translational diffusion contribution is by far the largest component in the fluctuations of scattering intensity; thus, one has to extract data from a very low signal-to-noise experiment. For molecules with size approaching the wavelength of light, rotational diffusion and structural changes contribute a sizable amplitude to the fluctuations, and their effect is easier to measure (4, 5). Yet the "coupling"[1] of translational, rotational and internal motions makes the interpretation complicated.

The characteristic dependence on scattering angle of the diffusional line width and the relative ease of obtaining contributions of other dynamic components extrapolated to low or high scattering angles have offered other approaches. This way the $\mathbf{q} \cdot \mathbf{v}$ Doppler-shifted spectrum (6–8) or q-independent contributions of rotational (4) and internal motion (5) were identified. Still, the use of extrapolations or multiparameter fits for resolving small components in the measured time correlation imposes severe experimental and mathematical requirements that make an unambiguous analysis of the contributions due to internal flexibility of the molecules, rotational motion, and structural changes of the scatterers difficult.

In this work we use cross-correlation for the separation of the translational diffusion from the other contributions to the dynamic fluctuations of laser light scattering. The use of direct differential measurements, can dramatically improve the accuracy and reliability of measurements, as compared with two separate measurements, as demonstrated elegantly for small differences in diffusional broadening by Cannell and Dubin (9). Translational diffusion fluctuations are eliminated by probing diffusional motion in a QELS experiment via changes in the amplitude of the Fourier transform of concentration fluctuations. The dependence of two Fourier components with wave vectors ($\mathbf{k}$) sufficiently close to each other creates the concept of the coherence solid angle of acceptance Δk_c, which is proportional to the inverse of the linear dimension of the scattering volume "seen" by the detector. In addition to the dynamics of diffusion, which is probed by the coherent laser light via the fluctuating Fourier pattern of the whole scattering volume, the dynamics of fluctuations due to rotation, internal motion, or chemical reaction can also be

[1]Coupling may be a misleading term for larger particles, as the rotational-translational Brownian motion is coupled also for small asymmetric molecules. It is only on the scale of distances of wavelength of light that this coupling is or is not detectable.

probed by a superposition of the fluctuating scattering intensities of each individual particle. Since the size of the scatterers is much smaller than the scattering volume, the latter fluctuations are correlated over a region Δk, which contains many coherence solid angles. Yet one can eliminate the fluctuations due to translational diffusion by cross-correlating the fluctuating intensities at two scattering angles that lie in different coherence solid angles.

Cross-correlation experiments were probably first performed by Brown and Twiss (10). The application of cross-correlation for determination of structures was proposed by us (11) for use with scattering from solutions of macromolecules. X rays and neutrons are capable of producing scattering patterns containing high-resolution structural data. The application of cross-correlation to light scattering is aimed at probing dynamic rather than structural data. An experimental demonstration of anticorrelation of scattering fluctuations was recently reported (12). The anticorrelation signal is an elegant and unambiguous demonstration of the principle, and was used to measure the rotational diffusion of long rodlike virus particles; we repeat it here in a somewhat different manner; other applications are also shown. It should be emphasized that the coherence of the laser is not required in the cross-correlation experiment. It is only its brightness that is used here. In fact, in a previous study, we used sunlight to measure the same fluctuations that were measured here (13). It could be mentioned also that cross-correlation of scattering intensity fluctuations from the same particles illuminated with two lasers with different colors could be used to design an equivalent experiment.

II. THEORY OF LIGHT SCATTERING CROSS-CORRELATION

The excess intensity of light scattered from a solution of N identical particles over that of the solvent scattering is given by:

$$I(\mathbf{k}, t) = \left| \sum_{j=1}^{N} f_j[\mathbf{k}, \alpha_j(t)] e^{i\mathbf{k}\cdot\mathbf{r}_j(t)} \right|^2, \tag{1}$$

where $\mathbf{k}$ is the scattering vector, $f_j[\mathbf{k}, \alpha_j(t)]$ is the scattering factor for the jth particle at position $\mathbf{r}_j(t)$, which depends on the scattering vector $\mathbf{k}$, and on the particle orientation and its conformation (or chemical state) which is symbolically denoted as $\alpha_j(t)$.

The cross-correlation function of the scattering intensities at two scattering angles with scattering vectors $\mathbf{k}_1$ and $\mathbf{k}_2$ is the time average (denoted as $\langle \cdots \rangle_t$) of the product of the instantaneous intensities of scattering at $\mathbf{k}_1$ and $\mathbf{k}_2$:

$$\begin{aligned} C(\mathbf{k}_1, \mathbf{k}_2, \tau) &\equiv \langle I(\mathbf{k}_1, t) I(\mathbf{k}_2, t+\tau) \rangle_t \\ &= \Big\langle \sum_{ijnm} f_i[\mathbf{k}_1, \alpha_i(t)] \\ &\quad f_j^*[\mathbf{k}_1, \alpha_j(t)] e^{i\mathbf{k}_1\cdot[\mathbf{r}_i(t)-\mathbf{r}_j(t)]} \\ &\quad \cdot f_n[\mathbf{k}_2, \alpha_n(t+\tau)] \\ &\quad f_m^*[\mathbf{k}_2, \alpha_m(t+\tau)] e^{i\mathbf{k}_2\cdot[\mathbf{r}_n(t+\tau)-\mathbf{r}_m(t+\tau)]} \Big\rangle_t \end{aligned} \tag{2}$$

Since the phases $\mathbf{k}\cdot\mathbf{r}_j(t)$ are totally random for different particles, the only terms that do not give a vanishing average on time are terms in which the indices i, j, n, and m contain at least two pairs of equal indices (references 14; 3, p. 94). Thus for $i = j$ and $n = m$ we obtain N^2 terms of the form

$$\langle |f_i[\mathbf{k}_1, \alpha_i(t)] f_n[\mathbf{k}_2, \alpha_n(t+\tau)]|^2 \rangle_t. \tag{3}$$

For $i = m$ and $j = n$ with $i \neq j$ we obtain $(N^2 - N)$ terms:

$$\begin{aligned} &\langle f_i[\mathbf{k}_1, \alpha_i(t)] f_i^*[\mathbf{k}_2, \alpha_i(t+\tau)] e^{i[\mathbf{k}_1\cdot\mathbf{r}_i(t)-\mathbf{k}_2\cdot\mathbf{r}_i(t+\tau)]} \\ &\quad \cdot f_j^*[\mathbf{k}_1, \alpha_j(t)] f_j[\mathbf{k}_2, \alpha_j(t+\tau)] e^{-i[\mathbf{k}_1\cdot\mathbf{r}_j(t)-\mathbf{k}_2\cdot\mathbf{r}_j(t+\tau)]} \rangle_t. \end{aligned} \tag{4}$$

and for $i = n$ and $j = m$ $(i \neq j)$ we have $(N^2 - N)$ terms of the form

$$\begin{aligned} &\langle f_i[\mathbf{k}_1, \alpha_i(t)] f_i[\mathbf{k}_2, \alpha_i(t+\tau)] e^{i[\mathbf{k}_1\cdot\mathbf{r}_i(t)+\mathbf{k}_2\cdot\mathbf{r}_i(t+\tau)]} \\ &\quad \cdot f_j^*[\mathbf{k}_1, \alpha_j(t)] f_j^*[\mathbf{k}_2, \alpha_j(t+\tau)] e^{-i[\mathbf{k}_1\cdot\mathbf{r}_j(t)+\mathbf{k}_2\cdot\mathbf{r}_j(t+\tau)]} \rangle_t. \end{aligned} \tag{5}$$

Terms in Eq. 5 vanish owing to an averaging of the initial phases of the particles. Terms in Eq. 4 give the translational diffusion correlation for $\mathbf{k}_1 = \mathbf{k}_2$. If, on the other hand, the two detectors are positioned such that $|\mathbf{k}_1 - \mathbf{k}_2| \gg (2\pi/A)$, A being the typical linear dimension of the volume seen by the detectors, this term is averaged to zero. This can be seen as follows:

$$\begin{aligned} &\mathbf{k}_1 \cdot \mathbf{r}_i(t) - \mathbf{k}_2 \cdot \mathbf{r}_i(t+\tau) \\ &\qquad = \mathbf{k}_1 \cdot [\mathbf{r}_i(t+\tau)] + (\mathbf{k}_1 - \mathbf{k}_2) \cdot \mathbf{r}_i(t+\tau). \end{aligned} \tag{6}$$

For short time differences, τ, the first term is contributing a small phase, which when averaged, yields the $e^{-\tau/2k^2D}$ decay to the autocorrelation funding, D, being the diffusion coefficient. The second term, though, is contributing a phase that is random, if the summation on positions $\mathbf{r}_i$ is covering a range much larger than $(2\pi/|\mathbf{k}_1 - \mathbf{k}_2|)$, i.e., if $\mathbf{k}_1$ and $\mathbf{k}_2$ are not in the same coherence area.

As a consequence, the only contributions to the cross-correlation that are not vanishing are terms in Eq. 3. Since $f_i[\mathbf{k}, \alpha_i(t)]$ is a smooth function of $\mathbf{k}$ over range $\Delta k \lesssim (2\pi/R,)$ R being the typical linear dimension of the particle, dynamical changes in $f_i[\mathbf{k}, \alpha_i(t)]$ due to the time dependence of $\alpha(t)$ can be detected by using the cross-correlation. To see this we can separate the term in Eq. 3 into an average component and fluctuations:

$$\delta|f_i[\mathbf{k}, \alpha_i(t)]|^2 = |f_i[\mathbf{k}, \alpha_i(t)]|^2 - \langle |f_i[\mathbf{k}, \alpha_i(t)]|^2 \rangle_t. \tag{7}$$

Thus,

$$\begin{aligned} &C(\mathbf{k}_1, \mathbf{k}_2, \tau) \\ &\quad = N^2 \{ \langle |f_i[\mathbf{k}_1, \alpha_i(t)]|^2 \rangle_t \langle |f_j[\mathbf{k}_2, \alpha_j(t)]|^2 \rangle_t \\ &\quad + \langle \delta|f_i[\mathbf{k}, \alpha_i(t)]|^2 \rangle \langle |f_i[\mathbf{k}_2, \alpha_j(t)]|^2 \rangle_t \\ &\quad + \langle |f_i[\mathbf{k}_1, \alpha_i(t)]|^2 \rangle_t \langle \delta|f_j[\mathbf{k}_2, \alpha_j(t)]|^2 \rangle_t \} \\ &\quad + (N^2 - N) \langle \delta|f_i[\mathbf{k}_1, \alpha_i(t)]|^2 \rangle_t \langle \delta|f_j[\mathbf{k}_2, \alpha_j(t)]|^2 \rangle_t \\ &\quad + N \langle \delta|f_i[\mathbf{k}_1, \alpha_i(t)]\ \delta|^2 f_i[\mathbf{k}_2, \alpha_i(t+\tau)]|^2 \rangle_t. \end{aligned} \tag{8}$$

All but the last term are independent of τ. If we take $\mathbf{k}_1$ and $\mathbf{k}_2$ close enough to assume

$$f_i[\mathbf{k}_1, \alpha_i(t)] = f_i[\mathbf{k}_2, \alpha_i(t)] \tag{9}$$

and we notice that

$$\langle \delta|f_i[\mathbf{k}, \alpha_i(t)]|^2 \rangle_t = 0, \tag{10}$$

we obtain a simplified expression for the cross-correlation:

$$\begin{aligned} C(\mathbf{k}, \mathbf{k}+\Delta\mathbf{k}, \tau) &= \{ N \langle |f_i[\mathbf{k}, \alpha_i(t)]|^2 \rangle_t |^2 \\ &\quad + N \langle \delta|f_i[\mathbf{k}, \alpha_i(t)]|^2\, \delta|f_i[\mathbf{k}+\Delta\mathbf{k}), \alpha_i(t+\tau)]|^2 \rangle_t. \end{aligned} \tag{11}$$

The second term is the term that gives the correlation function of the dynamics of changes of $\alpha_i(t)$. This correlation function is practically the autocorrelation for these dynamics, due to the smooth k-dependence of $f_i[\mathbf{k}, \alpha_i(t)]$. If α denotes the orientation of an asymmetric particle, ω, the cross-correlation will decay according to the rotational diffusion coefficient, D_R (12)

$$\langle \delta | f[\mathbf{k}, \omega(t)] |^2 \delta | f[\mathbf{k}', \omega(t+\tau)] |^2 \rangle_t$$
$$\propto \sum_l s_{l0}(k) s_{l0}(k') (2l + 1/2) P_l[\cos(\hat{kk'})]$$
$$\cdot \exp[-l(l+1)D_R\tau] \equiv A + Be^{-6D_R\tau} + Ce^{-20D_R\tau} + De^{-42D_R\tau} + \cdots \quad (12)$$

where $S_{l0}(k)$ are the spherical harmonic coefficients of the scattering intensity function (11) with the axis of rotational symmetry of the scattering particle taken at the z-direction; $\hat{kk'}$ is the angle between two scattering vectors. Tobacco mosaic virus (TMV) particles were the model system to measure this rotation. Numerical computations give the cofficients A, B, C, and D for TMV. They are, at 60°, 5.6, 2.8, 0.4, 0.05; at 90°, 4.6, 3.2, 1.1, 0.2; and at 120°, 3.9, 3.1, 1.4, 0.4, respectively.

The second problem we chose to study using the cross-correlation approach is the measurement of the dynamics of internal motion of long-coil DNA molecules in solution. The fluctuations in the scattering factor in this case are due to intramolecular interference changes reflecting the relative motion of segments along the DNA molecule. This internal interference depends on the scattering wavelength both by its amplitude and its correlation time (15–18). Dependence that follows k^2 (19) and k^3 (20) was predicted theoretically.

The last set of measurements was done with a solution of lysozyme molecules in NaCl, a mixture that is used for lysozyme crystallization and was shown (21) to grow a wide range of aggregate sizes that maintain a quasi-equilibrium because of the nucleation barrier in which spontaneous fluctuations due to association-dissociation kinetics take place. In this case the scattering factor is directly proportional to the number of monomers in each aggregate.

The kinetics of the aggregation reactions are of crucial importance for crystal growth processes, and were measured by us using temperature and pressure jump techniques.[2] Reaction kinetics were measured from fluctuations in charges (22). The use of light scattering for measurement of aggregation reaction kinetics by light scattering was suggested long ago (2, 23–26) but the signal for laser-scattering autocorrelation experiments was estimated to be immersed in the signal because of diffusion.

III. SIGNAL-TO-NOISE RATIO AND DESIGN OF EXPERIMENTS

Evaluation of the predetection signal-to-noise ratio was described in detail for the measurements of the spatial correlation with x rays (11). Since intensity fluctuations from all scatterers are independent, they add randomly and the correlation signal is proportional to the concentration. The noise due to photon counting statistics of the time-averaged intensity is also proportional to the concentration; thus signal-to-noise ratio is independent of concentration. This ratio is proportional to the average number of photons detected during one correlation decay time from each scatterer, and to the relative fluctuations mean square from each scatterer. In order to detect the maximal number of photons scattered from each particle, optimization of the cross-correlation signal for light implies maximal incident flux and largest collection aperture. This is achieved by focusing the laser and by using a microscope objective with large aperture for the detection of the scattering intensity fluctuations. Using a microscope objective also enables one to image the illuminated volume with high magnification and select a very small scattering region to be seen by the detectors, thus increasing the relative fluctuations. The same objective is used to image the scattering volume to both detectors. The two halves of the aperture, which correspond to different scattering angles, are divided behind a pinhole positioned at the image plane.

Since the signal-to-noise ratio of fluctuations due to translational diffusion is proportional to the concentration of the scattering particles (14), whereas the signal-to-noise ratio of cross-correlation fluctuations is independent of concentration, low concentrations are advantageous. Also, the collection of many coherent areas increases the signal-to-noise ratio of the cross-correlation because of the increasing number of total detected photons per particle. However, the autocorrelation signal due to concentration fluctuations is independent of the number of coherent areas detected, since it is proportional to the number of detected photons per coherent area (14).The cross-correlation experiment is therefore designed to collect the scattering with large apertures from a very dilute solution.

The size of the scattering volume is mainly determined by the requirement that the dynamics of number fluctuations will be considerably slower than the cross-correlation decay time of interest. We found that slow turbulent flows in the cell, rather than pure translational diffusion, are the dominant processes of exchange of particles in the small volume seen by the detectors. Using spherical polystyrene latex particles we found that a linear dimension of 0.1 mm results in a number-fluctuation-correlation time on the order of 0.1 s when standard spectroscopic cells were used. This time could be made longer using smaller flow cells, probably resulting from the reduction in turbulence due to smaller temperature gradients and larger friction with the walls.

The experimental system is schematically described in Fig. 1. It includes micrometric adjustments of all the optical components to achieve high laser flux by focusing with a 5-mm lens, to obtain sharp imaging of the scattering volume on the pinhole and to split the microscope objective aperture. In the first stage of the experiments the scattered light was split just behind the microscope lens and focused on two slits in front of the two photomultipliers. This setup required cumbersome adjustments to make the two detectors see the same scattering volume. This step is avoided in the present arrangement, in which the pinhole first selects the scattering volume and then splits the scattered light.

The detection and electronic system consists of two 8850 RCA photomultipliers (RCA Electro-Optics & Devices, Lancaster, PA), fast amplifiers and discriminators, and a multibit Malvern correlator, type K 7025 (Malvern Instruments, Great Malvern, Wore., England). Clipped photon correlators are fast and accurate if applied for the analysis of large fluctuations. Since clipping or scaling is used in such correlators, the enhancement of fluctuations that contribute only a small component to

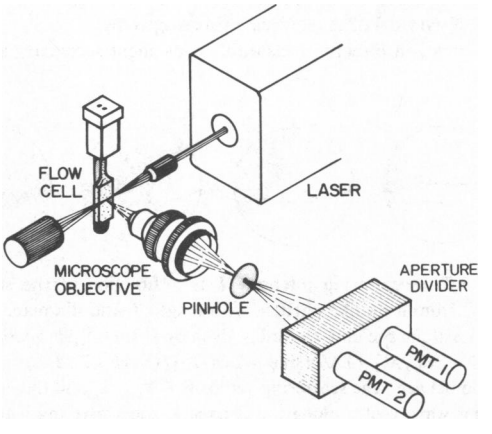

FIGURE 1 The optical system. An Argon ion laser beam is focused in a spectroscopic flow cell filled with a solution of scattering particles. A microscope objective images the scattering volume on a pinhole. The two halves of the objective aperture are then divided to the two cross-correlated photomultiplier detectors.

[2]Unpublished results are partially presented in Fig. 5 *b* and *c*.

the total signal becomes very inefficient. For TMV the 4-bit Malvern correlator was found reasonably effective even with prescaling of 2^7. The speed of hard-wired digital fast Fourier transformers allows for efficient accumulation of power spectra, which enhances information equivalent to the correlation function with precision determined by the digital accuracy of the input, which is close to the quantum limit in the case of photon counting. We are now successfully using photon counters interfaced to a UNIGON 4520 dual-channel FFT processor (Unigon Industries, Mount Vernon, NY) with 12 bits input, and 1,024 channels to improve the accuracy of our results.

The choice of TMV for demonstrating the use of the cross-correlation for the measurement of rotational diffusion coefficient is illustrated in Fig. 2. Here we illustrate the scattering intensity pattern of a single TMV particle as detected on a sphere around it, as a function of its orientation, using green light. The pattern is basically a cone of strong scattering at the reflection angle from the long axis of the TMV, which results in large fluctuations in scattering intensity because of the rotational diffusion. The width of the scattering cone (given by the inverse length of the virus) is 20–30°, which sets the required apertures of acceptance of the scattered light for the detectors, as well as the maximum separation between them. This feature in the scattering of TMV was used in the anticorrelation experiment of Griffin and Pusey (12), in which two detectors were positioned in opposite directions at 90° scattering angles.

The evaluation of the signal-to-noise ratio for the experiments requires an estimation of the number of detected photons per particle during one correlation decay time. The scattering intensity per particle, I/N can be calculated from (27)

$$I/N = I_B/V \cdot M^2 \cdot P(\theta) \cdot \left(\frac{4\pi^2 n_B^2}{\lambda_0^4 N_A^2 R_B}\right)\left(\frac{\partial n}{\partial c}\right)^2 = I_B/V \cdot M^2 \cdot P(\theta) \cdot (3.35 \times 10^{-26}), \quad (13)$$

where $n_B = 1.511$, $R_B = 29.9 \times 10^{-6}\ \text{cm}^{-1}$ and I_B/V are, respectively, the refractive index of benzene, its Rayleigh ratio, and the number of scattered photons detected per unit volume of benzene used here as a secondary standard; $\lambda_0 = 5{,}145$ Å is the wavelength of the laser light, N_A is Avogradro's number, $(\partial n/\partial c) \sim 0.17\ \text{cm}^{-3}$ is the index of refraction increment due to the dissolved particles, M their molecular weight, and $P(\theta)$ the normalized scattering factor which is the ratio of scattering intensity at angle θ to the forward scattering intensity. Using the limiting Zimm slope approximation we can write (27)

$$P^{-1}(\theta) \sim [(R_G \cdot 4\pi n)/\sqrt{3}\lambda_0] + 1 = (R_G/529)^2 + 1 \quad (14)$$

where $n = 1.34$ is the index of refraction of the scattering solution and R_G the radius of gyration of the molecule (in Ångstroms).

I_B/V, which is a directly measurable convenient secondary standard, includes the laser flux, scattered light collection aperture, and quantum efficiency of detection. For $V = 10^{-6}\ \text{cm}^3$, with a laser focused to 0.1 mm beam diameter and with a collection aperture of 0.85 steradians using a microscope objective, we can easily obtain a value of

$$I_B/V = 2 \times 10^{15}\ \text{photons/s/cm}^3. \quad (15)$$

This means that for TMV with $M = 6 \times 10^7$ daltons, $R_G = 866$ Å (for a 3,000-Å long rod), and $P(90°) \sim 0.27$,

$$I_{TMV}/N = 6 \times 10^4\ \text{photons/s/particle}. \quad (16)$$

At correlation decay times of the order of a millisecond, many photons can be detected from each particle, giving a high signal-to-noise ratio.

For the *Escherichia coli* plasmid DNA with $M = 4 \times 10^6$, $R_G = 2{,}000$ Å, and $P(90°) \sim 0.066$ (28),

$$I_{DNA}/N = 70\ \text{photons/s/particle}. \quad (17)$$

This gives a signal-to-noise ratio of the order of 0.1, which can be improved by finer focusing of the laser, as was done.

The value of I/N for lysozyme aggregates in a crystallization mixture $I/N \sim 7 \times 10^{-3}$ photons/s/particle. This value increases to 0.7 for 10-mers. Since the correlation time is about 0.1 s we can expect a reasonably high signal-to-noise ratio because of the dynamics of association-dissociation of the larger aggregates.

The final, postdetection signal-to-noise ratio achieved in an experiment is given by the product of the predetection signal-to-noise ratio and the square root of the number of correlation times during which the data were collected. It is the direct evaluation of the ratio of the correlation signal amplitude and noise of the photon-counting statistics in this signal. Since other noise sources can be present, it is the best possible estimate for the quality of the results.

In contrast to the signal-to-noise ratio, the ratio of the signal to the background (the correlation base line) is inversely proportional to the number of scatterers in the beam, and directly proportional to the relative mean-square fluctuation in scattering intensity from each particle ($\langle\langle\delta|f^2|^2\rangle\rangle/\langle|f^2|^2\rangle$ in Eq. 11). It is independent of the duration of the experiment. The ratio of the signal to the background and to the photon statistical noise as given by the square root of the background offers a check on the experimental results.

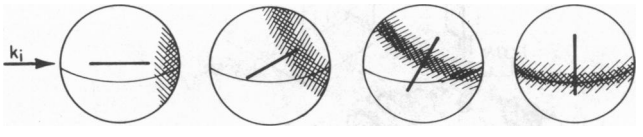

FIGURE 2 The scattering intensity I as a function of the scattering angles $(\theta\phi)$ from a rodlike particle with length L and diameter d whose long axis lies along the unit vector $\mathbf{l}$ is given by $I(\theta\phi) = \{[\sin(\cos\psi \cdot 2\pi L/\lambda)]/[(\cos\psi \cdot 2\pi L/\lambda)] \cdot [2J_1(\sin\psi \cdot 2\pi d/\lambda)]/(\sin\psi \cdot 2\pi d/\lambda)]^2$, where ψ is the angle between the scattering vector $\mathbf{K} = \mathbf{k}_i - \mathbf{k}_s$ and the vector $\mathbf{l}$, $\mathbf{k}_i$ the incident wave vector along the Z axis, $\mathbf{k}_s$ the scattering wave vector (angles $\theta\phi$) and λ the radiation wavelength. The scattering intensity is presented schematically by the degree of shadowing on a unit sphere as a function of $\theta\phi$ for different orientations of the rod as plotted with $L = 3{,}000$ Å, $d = 150$ Å and unpolarized green light. Polarization perpendicular to equator marked on the sphere introduces the $\cos^2$ additional factor which we did not attempt to shadow for clarity.

IV. MATERIALS

TMV particles were given to us by Dr. M. Bar Joseph from the Virus Laboratory of the Volcani Agricultural Research Center, Bet Dagan, Israel. The *E. coli* plasmid DNA was prepared in our laboratory according to the procedure described elsewhere (28) in its circular supercoiled form and was cut open by the restriction enzyme EcoRI, to obtain the linear form that we used.

Lyophilized lysozyme from the Worthington Biochemical Corp. (Freehold, NJ) was dissolved in acetic acid buffer, pH 4.2. An 8% wt/vol protein solution was mixed with an equal volume of 10% NaCl to obtain the supersaturated mixture. This solution grows visible crystals within 1 h.

V. RESULTS

In Fig. 3 we plot the cross-correlation measured from the scattering of TMV particles at 22°C. The data presented were accumulated during a few minutes. A fraction of a minute was enough to see the cross-correlation rising above the noise. The correlation time was measured as a function of the scattering angle, and was found to be constant within the experimental error. The angular-dependence data were collected using a cylindrical cell. The cylindrical optics causes a detectable deterioration in the laser focusing,

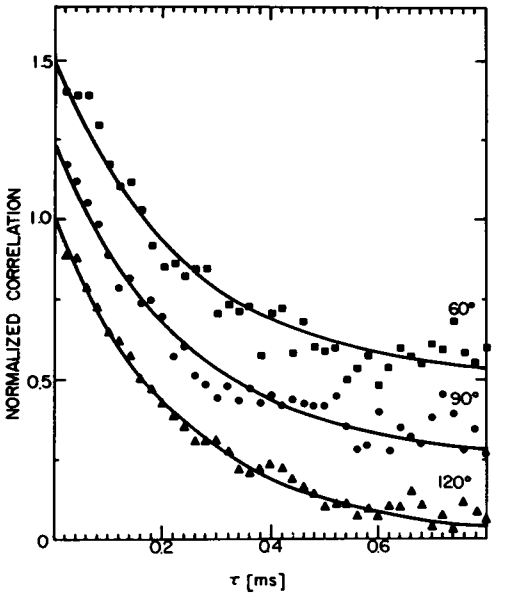

FIGURE 3 Cross-correlation measured from TMV scattering. The fitted correlation time of 240 ± 20 μs, independent of scattering angle. The correlation at 90° and 60° are shifted along the ordinate by 0.25 and 0.5 units, respectively.

which decreased the signal-to-noise ratio as expected. The cross-correlation signal also deteriorates when the pinhole behind the collecting microscope objective is shifted, even very slightly, away from the image plane. These tests confirm the source of the correlation signal. The quality of the results is determined by the laser noise, notably 50-Hz harmonics.

The signal-to-background ratio is 0.002, compatible with ~100 particles in the beam, and 20% relative mean-square fluctuations per particle. The total of 2×10^6 photons/s implies 2×10^4 photons/s scattered from one TMV particle, in accordance with Eq. 16.

The data were fitted using the cumulant method, with one cumulant. Since number fluctuations show up at longer sample times, with a correlation time of a few hundred milliseconds, a rather flat base-line results. A Fibonacci search for best-fitted base line coincided, within statistical error, with the base line measured using the delayed channels. The relaxation times at 60°, 90°, and 120° were all fitted with a decay time of 0.24 ± 0.03 ms. Using Eq. 12 and the numerical computations of the coefficients for TMV, a best single-exponential decay of ~7.5 D_R, 9.5 D_R, and 11 D_R should fit the data at 60°, 90°, and 120° scattering angles, respectively, whereas the experimental fit gives ~12 D_R. We repeated the measurements for two samples of TMV particles. The radius of gyration was measured by total-intensity light scattering to be 860 and 750 Å. Electron microscopic examination reveals a fraction of broken particles in the second sample. Although the radius of gyration and the diffusion coefficient of heterogenous solutions produce different averages of the length distribution of the particles, one expects to detect ~30% increase in the rotational diffusion coefficient of the second sample. Indeed the decay time measured was 0.17 ms.

In Fig. 4 we show the cross-correlation obtained by scattering laser light from *E. coli* plasmid DNA molecules. The dynamics of the scattered light intensity fluctuations is associated with segmental diffusion motion of the DNA coil (15). So far these relaxation times have been deduced from a rather indirect analysis of homodyne scattering experiments, which include the contribution of the translational diffusion fluctuations (5, 16–18, 28). Unlike the correlation due to rotational diffusion relaxation of rigid molecules, the measured correlation due to internal degrees of freedom depends on the scattering vector length. We measured the cross-correlation signal at 60°, 90°, and 120°. The correlation signal-to-noise ratio is here smaller, as was estimated. The relaxation times scale rather well with the third power of the scattering vector. They are comparable to the autocorrelation decay times in corresponding angles (29), which confirms the dominant contribution of the diffusional motion of segments along the DNA coil. The signal-to-background ratio of 2×10^{-6} is compatible with 2×10^4 molecules in the beam, 4% relative mean-square fluctuations per particle, and 100 photons/s scattered from each DNA molecule. Since ~10^6 correlation times were accumulated, a postdetection signal-to-noise ratio of 100 would ideally be expected, but periodical laser noise correlation causes this ratio to deteriorate to ~10.

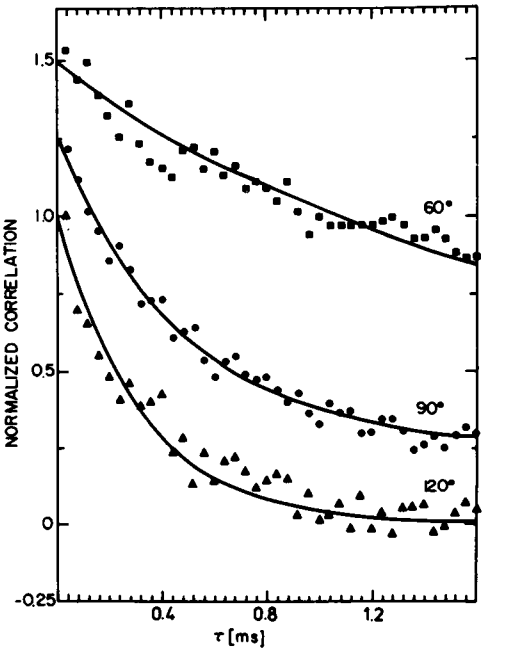

FIGURE 4 Cross-correlation of fluctuation scattering from *E. coli* plasmid DNA molecules. The fitted correlation times are 400, 120, and 80 μs at scattering angles of 60°, 90°, and 120°, respectively. The correlations at 90° and 60° are shifted along the ordinate by 0.25 and 0.5 units, respectively.

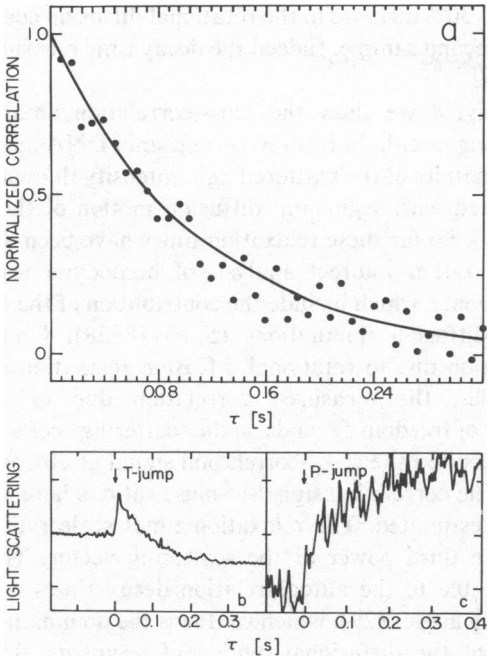

FIGURE 5 Cross correlation obtained from the analysis of the scattering from supersaturated lysozyme and NaCl mixture. The correlation time of 112 ms was also measured by light-scattering intensity during temperature and pressure jumps, and presented in *b* and *c*, respectively. The temperature jump was carried out in the laboratory of Prof. I. Pecht at the Weizmann Inst., and the pressure jump in Prof. Gutfreund's laboratory in Bristol, England.

Fig. 5 *a* is the cross-correlation measured from a solution of 4% lysozyme in 5% NaCl, pH 4.2. The correlation time of ~0.1 s is in agreement with relaxation times of light-scattering intensity from the same solution measured by temperature and pressure jump techniques presented in Fig. 5 *b* and *c*. The rate and amplitude of the cross-correlation implies that it is mainly contributed by the slow fluctuations in size of the large aggregates. The rate of crystal nucleation and growth estimated using the measured equilibrium constants of aggregation of this system (21) agrees well with our experimental observation.[2]

VI. CONCLUSIONS

In this work we applied cross-correlation of scattering-intensity fluctuations at two scattering angles for a direct measurement of rates of processes that contribute to fluctuations in light-scattering intensity. They are dominated in the autocorrelation analysis by relaxation of concentration fluctuations of the scatterers due to the translational diffusion.

The measurements of the rotational diffusion of TMV particles indicate that this method is practical for studying large asymmetric scatterers. The much higher sensitivity of rotational diffusion to size, as compared with the translational diffusion coefficient, compensates for the lower signal-to-noise ratio and makes the effort required to perform the cross-correlation experiment well worth it. The increased difficulties of total-intensity light-scattering measurements of large particles at low scattering angles and the coupling of translational and rotational diffusion contributions to the usual quasi-elastic light scattering autocorrelation experiment further support this conclusion. Applications of the cross-correlation technique to studies of assemblies that form elongated structures (e.g., actin filaments and microtubules) and of motile systems seem quite appealing. However, one lacks a simple relation between the measured correlation and the rotational diffusion, since the relaxation time depends on higher spherical harmonic expansion coefficients as the scatterers's dimension approach the wavelength of light. Referring to Fig. 2 it is easily realized that the light-scattering relaxation time depends on the detailed profile of the scattering pattern, and not only on the rotational diffusion.

The probing of the dynamics of conformational changes by cross-correlation gives a direct measurement of relaxation times, whereas separation of these data from the autocorrelation necessitates also the determination of their amplitudes using multiparameter-fit procedures. The possibility of cross-correlating polarized and depolarized scattering fluctuations may further elucidate dynamic contributions of internal motion. Although there is additional information in measurements of the cross-correlation as a function of the angle between the two detectors for determining the flexibility of long coils, in practice, only a limited range of **k** vectors is accessible to such analysis.

Measurements of the kinetics of aggregation reactions are of interest, since the probing of kinetic parameters in unperturbed systems has many advantages for studies of interacting biological particles. We conclude that laser cross-correlation studies are feasible when the theoretical signal-to-noise ratio is high enough. However, the cleaning-up of the sample is even more crucial than in other light scattering studies; this can be handled by careful filtering or centrifugation. Laser noise, especially 50-Hz harmonics, is a major obstacle in improving the data. The use of electronic compensators or the identification of these harmonics in the cross-power spectrum offer the means for significant reduction of laser noise contributions.

Finally, we have tried to minimize the effect of number fluctuations in our experiments by keeping the exchange of particles in the scattering volume very slow. As shown in previous studies (30, 31) it is possible to reduce the scattering volume by an order of magnitude, and increase artificially the flow of particles through the scattering volume. This would permit measuring the number and size of particles in the scattering volume.

We should like to acknowledge the suggestions of and stimulating discussions with Dr. S. Reich and Prof. H. Eisenberg, and the help of Drs. H. Gutfreund and I. Pecht in the lysozyme aggregation kinetic experiments. We thank L. Wallerman for machining the optical parts.

The instrumentation was funded by K. and A. Wallenberg Stiftelsen. The research was partially supported by a grant from the United States-Israel Binational Science Foundation, Jerusalem, Israel.

Dr. Kam is the incumbent of the Pollak Career Development Chair.

Received for publication 5 February 1981 and in revised form 25 January 1982.

REFERENCES

1. Chu, B. 1974. Laser Light Scattering. Academic Press, Inc., New York.
2. Berne, B. J., and R. Pecora. 1976. Dynamic Light Scattering. John Wiley & Sons, New York.
3. Cummins, H. Z., and E. R. Pike, editors 1977. Photon Correlation Spectroscopy and Velocimetry. NATO Advanced Study Institutes Series. Plenum Publishing Corp., New York.
4. Cummins, H. Z., F. D. Carlson, T. J. Herbert, and G. Woods. 1969. Translational and rotational diffusion constants of tobacco mosaic virus from rayleigh linewidths. *Biophys. J.* 9:518–546.
5. Jolly, D. and H. Eisenberg. 1976. Photon correlation spectroscopy, total intensity light scattering with laser radiation, and hydrodynamics studies of a well fractionated DNA Sample. *Biopolymers.* 15:61–95.
6. Ware, B. R. and W. H. Flygare. 1971. The simultaneous measurement of the electrophoretic mobility and diffusion coefficient in bovine serum albumin solutions by light scattering. *Chem. Phys. Lett.* 12:81–85.
7. Ware, B. R., and W. H. Flygare. 1972. Light scattering in mixtures of BSA, BSA dimers, and fibrinogen under the influence of electric fields. *J. Colloid Interface Sci.* 39:670–675.
8. Uzgiris, E. E. 1974. Laser Doppler Spectrometer for study of electrokinetic phenomena. *Rev. Sci. Instrum.* 45:74–80.
9. Cannell, D. S., and S. B. Dubin. 1975. Differential light scattering technique for the study of conformational changes in macromolecules. *Rev. Sci. Instrum.* 46:706–712.
10. Brown, R. H. and R. Q. Twiss. 1956. Correlation between photons in coherent light rays. *Nature (Lond.)* 178:1447–1448.
11. Kam, Z. 1977. Determination of macromolecular structures in solution by spatial correlation of scattering fluctuations. *Macromolecules.* 10:927–934.
12. Griffin, W. G., and P. N. Pusey. 1979. Anticorrelations in light scattered by nonspherical particles. *Phys. Rev. Lett.* 43:1100–1104.
13. Reich, S., and Z. Kam. 1979. Sunlight scattering intensity fluctuations from asymmetric particles. *Opt. Comm.* 30:293–298.
14. Clark, N. A., J. H. Lunacek, and B. Benedek. 1970. A study of Brownian motion using light scattering. *Am. J. Phys.* 38:575–585.
15. Pecora, R. 1968. Spectral distribution of light scattered from flexible-coil macromolecules. *J. Chem. Phys.* 49:1032–1035.
16. Caloin, M., B. Wilhelm and M. Daune. 1977. Quasielastic light scattering: effect of ionic strength on the internal dynamics of DNA. *Biopolymers.* 16:2091–2104.
17. Schmitz, K. S. 1979. Quasielastic light scattering by biopolymers. III. Effect of ionic strength on internal dynamics of DNA. *J. Mol. Biol.* 123:539–555.
18. Thomas, J. C., S. A. Allison, J. M. Schurr, and R. D. Holder. 1980. Dynamic light scattering studies of internal motion in DNA. *Biopolymers.* 19:1451–1474.
19. Lin, S. C. and J. M. Schurr. 1978. Dynamic light-scattering studies of internal motions in DNA. I. Application of the Rouse-Zimm model. *Biopolymers.* 17:425–461.
20. Debois-Violette, E., and P. G. deGennes. 1965. Quasielastic scattering by dilute, ideal, polymer solutions. *Physics.* 3:181–198.
21. Kam, Z., H. B. Shore, and G. Feher. 1979. On the crystallization of proteins. *J. Mol. Biol.* 123:539–555.
22. Feher, G., and M. Weissman. 1973. Fluctuation spectroscopy: determination of chemical reaction kinetics from frequency spectrum of fluctuations. *Proc. Natl. Acad. Sci. U. S. A.* 70:870–875.
23. Berne, B. J., and H. L. Frisch. 1967. Light scattering as a probe of fast reaction kinetics. *J. Chem. Phys.* 47:3675–3676.
24. Blum, L. 1969. Light scattering from reactive fluids. III. Intensity calculation. *J. Chem. Phys.* 51:5024–5028.
25. Bloomfield, V., and J. A. Benbasat. 1971. Inelastic light scattering study of macromolecular reaction kinetic. I. *Macromolecules.* 4:609–617.
26. Benbasat, J. A., and V. Bloomfield. 1973. Inelastic light scattering study of macromolecular reaction kinetics II. *Macromolecules.* 6:593–597.
27. Tanford, C. 1961. Physical Chemistry of Macromolecules. John Wiley & Sons, New York. Chap. 5.
28. Voordouw, G., Z. Kam, N. Borochov, and H. Eisenberg. 1978. Isolation and physical studies of the intact supercoiled, the open circular and the linear forms of ColE$_1$-Plasmid DNA. *Biophys. Chem.* 8:171–189.
29. Kam, Z., N. Borochov, and H. Eisenberg. 1981. Dependence of laser scattering of DNA on NaCl concentration. *Biopolymers.* 20:2671–2690.
30. Weissman, M., H. Schindler, and G. Feher. 1976. Determination of molecular weights by fluctuation spectroscopy: application to DNA. *Proc. Natl. Acad. Sci. U. S. A.* 73:2776–2780.
31. Magde, D. 1977. Concentration correlation analysis and chemical kinetics. *In* Molecular Biology, Biochemistry and Biophysics. I. Pecht and R. Rigler, editors. Vol. 24. Springer-Verlag, Heidelberg. 43–83.